Journal of Non-Crystalline Solids 354 (2008) 3747–3751

Contents lists available at ScienceDirect

Journal of Non-Crystalline Solids

journal homepage: www.elsevier.com/locate/jnoncrysol

Spectroscopic properties of Er^{3+}-doped $xGeO_2$–$(80-x)TeO_2$–10ZnO–10BaO glasses

Yanmin Yang [a,b,c], Baojiu Chen [a,b,*], Cheng Wang [b], Guozhong Ren [b], Qingyu Meng [a,b], Xiaoxia Zhao [a,b], Weihua Di [b,c], Xiaojun Wang [b], Jiashi Sun [a], Lihong Cheng [a], Tao Yu [a], Yong Peng [a]

[a] Department of Physics, Dalian Maritime University, Dalian 116026, PR China
[b] Lab of Excited State Processes, Changchun Institute of Optics, Fine Mechanics and Physics, Chinese Academy of Sciences, Changchun 130033, PR China
[c] Graduate School of the Chinese Academy of Sciences, Beijing 100039, PR China

ARTICLE INFO

Article history:
Received 10 May 2007
Received in revised form 7 March 2008
Available online 13 May 2008

PACS:
73.61.Jc
74.25.Bt
74.25.Gz

Keywords:
Glasses
Heavy metal oxides
Optical spectroscopy
Absorption
Luminescence
Germanates
Tellurites
Rare-earths in glasses

ABSTRACT

Erbium-doped glasses with composition $xGeO_2$–$(80-x)TeO_2$–10ZnO–10BaO were prepared by melt-quenching technique. The phonon sideband spectra and the optical absorption band edges for the host matrix were confirmed by means of the spectral measurements. Standard Judd–Ofelt calculations have been completed to these glasses. The dependence of up-conversion and infrared emission under 980 nm excitation on the glass composition was studied. The quantum efficiencies for the $^4I_{13/2} \rightarrow {}^4I_{15/2}$ transition of trivalent erbium in the glasses were estimated.

1. Introduction

Due to the rapid growth of information superhighway and the need for flexible networks, optical amplifiers with a wide and flat gain spectrum in 1.5 μm telecommunication window are required [1–4]. Tellurite-based erbium-doped fiber amplifiers (EDFAs) have attracted considerable attention because of over 70 nm broad bandwidth. However, the lower phonon energy of tellurite glass leads to serious up-conversion emission and decreases the efficiency of 1.5 μm emission. GeO_2 has long been recognized as a good glass former [5]. GeO_2 based glasses have higher phonon energy, better thermal stability and infrared transmission than the tellurite-based glasses. Recently, some of investigations have focused on the tellurium-germanate glasses. Chun Jiang and his coworkers reported the emission properties of trivalent ytterbium in GeO_2–TeO_2 glasses [6]. Xian Feng et al. reported the effect of composition and various preparation procedures on the content and vibration frequency of hydroxyl groups in Er^{3+}-doped GeO_2–TeO_2–ZnO–NaO–Y_2O_3 glasses [7]. Pan and Morgan reported on optical transition of tellurium-germanate glasses $(63-x)GeO_2$–$xTeO_2$–27PbO–10CaO, $x = 0$–40 [8]. However, to our best knowledge there is no a detailed study on the infrared emission properties of Er^{3+} in the GeO_2–TeO_2–ZnO–BaO glass system. It is expected that introducing proper amount of GeO_2 into the telluride glass could improve the glass mechanical and thermal performance, meanwhile, could reduce up-conversion emission and increase pump efficiency.

In this paper, the optical transition of Er^{3+}, the phonon sideband and optical band edge for the host matrix, and the dependence of quantum efficiency on the glass composition were studied.

2. Experimental

2.1. Sample preparation

Glasses with various composition $xGeO_2$–$(80-x)TeO_2$–10ZnO–10BaO–$0.5Er_2O_3$ (GEEr) or $1Eu_2O_3$ (GTEu) ($x = 0$–80, with an increment of 10; if without specific statement below, x represents the

* Corresponding author. Address: Department of Physics, Dalian Maritime University, Dalian 116026, PR China. Tel./fax: +86 411 84728909.
E-mail address: chenmbj@sohu.com (B. Chen).

0022-3093/$ - see front matter © 2008 Elsevier B.V. All rights reserved.
doi:10.1016/j.jnoncrysol.2008.03.047

same meaning) were prepared by using analytical grade GeO_2, TeO_2, ZnO, $BaCO_3$ and Er_2O_3 or Eu_2O_3 as starting materials. Eu^{3+}-doped GTEu samples were prepared for obtaining the phonon sideband. According to the designed composition the starting materials were weighed and well mixed together. Each batch was put into an alumina crucible and heated in an electronic muffle furnace at around 1200 °C for 30 min. The melted mixture was then poured on a preheated brass mold to form glass disks. After 15 h-annealing at 300 °C, the sample was cut and polished for the spectral measurements. The temperature accuracy for the system is ±5 °C. Table 1 shows the sample numbers, glass compositions and some basic physical characteristics.

2.2. Optical and spectroscopic measurements

Refractive indexes of all the samples were measured by using an UVISEL SPME of ellipsometry. The measurement accuracy of refractive index is ±0.01. Densities were measured according to Archimedes' principle using distilled water as the medium. The absolute uncertainty for the densities was estimated by the error transfer principle to be less than ±0.1 g/cm^3. The Er^{3+} concentrations and molar volumes were estimated based on the designed composition and the measured volumes. These results were shown in Table 1. The glass transformation temperature (T_g) and crystallization onset temperature (T_x) were measured using a differential thermal analysis (DTA) with a heating rate of 10 °C/min. The measurement accuracy of temperature is ±1 °C. The absorption spectra for all the Er^{3+}-doped samples were obtained at a Shumandzu\UV\3101PC double beam spectrophotometer in the range of 200–1700 nm at room temperature. In these measurements the wavelength accuracy is ±0.3 nm at UV/VIS and ±1.6 nm at NIR. The excitation spectra for the Eu^{3+}-doped glass samples were measured with a Hitachi F4500 fluorescence spectrophotometer, while monitoring the $^5D_0 \rightarrow {}^7F_2$ emission at 612 nm. The measurement accuracy of wavelength is ±2 nm, wavelength resolution is 1.0 nm. The up-conversion emission, infrared emission spectra, fluorescence decays of Er^{3+}:$^4I_{13/2} \rightarrow {}^4I_{15/2}$ were measured by using the 980 nm pulsed output of an OPO laser (Continue/Sunlite-8000) as excitation light. The fluorescent signals were collected and processed via a spectrometer (Triax 550) equipped with a semiconductor detector controlled by a personal computer. In these measurements the wavelength accuracy is ±0.06 nm, and the wavelength resolution is 0.002 nm.

3. Results

All the prepared samples with various compositions look better transparent and uniform that indicated all the designed compositions fall into the glass formation range of this quaternary system. It is also found that all the samples show the body color to be pink or red due to the Er^{3+} or Eu^{3+} doping. We have tried to replace BaO with different amounts of Na_2O, and then the new glasses with better quality were also obtained. These facts show us that this quaternary system is featured with wider glass formation range and stronger glass-forming ability.

In order to evaluate thermal stability the DTA was completed to the glass samples xGeO$_2$–(80 − x)TeO$_2$–10ZnO–10BaO–0.5Er$_2$O$_3$ (here x = 0, 20, 40, 60 and 80). The DTA curves are shown in Fig. 1. In this figure T_g represents the glass transition temperature, T_x denotes the crystallization onset temperature. It can be seen that as x, namely, content of GeO_2 increases, T_g monotonously increases from 340 °C (for the ternary system: 80TeO$_2$–10ZnO–10BaO, namely GT08) to 590 °C (for another ternary system 80GeO$_2$–10ZnO–10BaO, namely GT80). The low T_g of this tellurite glass is a drawback to its application in optical waveguide produced with ion-exchange, since the ion-exchange usually is accomplished at around 300 °C [9]. As is seen GeO_2 introduction can increase T_g and would make the glass satisfy the ion-exchange technique. Fig. 1 indicates also the change of the crystallization onset temperature while the glass composition is varied. The glass containing 60% of GeO2 and 20% TeO_2 displays highest crystallization onset temperature. The glass GT08 and GT80 exhibit sharp exothermal peaks at about 550 °C and 750 °C, respectively. These peaks imply strong crystallization when the samples experience these temperatures. For other samples containing both the components TeO_2 and GeO_2, the exothermal peaks will appear at higher temperatures then 750 °C. The temperature difference $\Delta T = T_x - T_g$, in general, is a sign of the stability for the glass. The larger the ΔT the better is the stability of the glass. To achieve a large range of working temperature during the fiber drawing, it is desired that the glass host has as large ΔT as possible [10,11]. From Fig. 1 it can be seen that with an increase of introducing GeO_2-content into

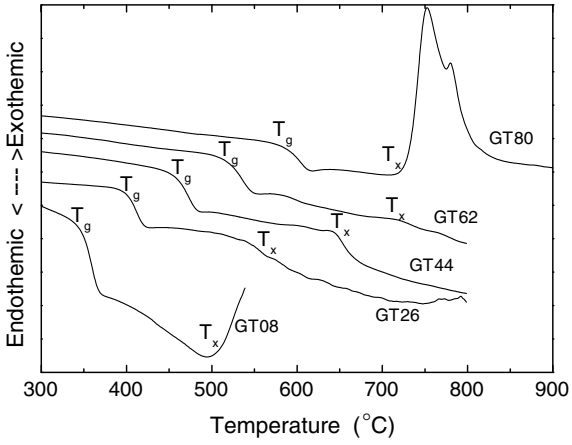

Fig. 1. Glass transition temperature T_g, crystallization onset temperature T_x, in xGeO$_2$–(80 − x)TeO$_2$–10ZnO–10BaO glasses (x = 0–80 mol%).

Table 1
Refractive indexes, densities, Er^{3+} concentrations and mole volumes of xGeO$_2$–(80 − x)TeO$_2$–10ZnO–10BaO glasses (x = 0–80)

Compositions	GeO_2 (mol%)	TeO_2 (mol%)	ZnO (mol%)	$BaCO_3$ (mol%)	Er_2O_3 (mol%)	Density (g/cm^3)	Mole volume (cm^3/mol)	Er^{3+} content 1×10^{20}	Refractive indexes
Uncertainty	±0.01	±0.01	±0.01	±0.01	±0.01	±0.1	±0.1	±0.1	±0.01
GT08	0	80.00	10.00	10.00	0.50	5.5	29.7	2.0	1.98
GT17	10.00	70.00	10.00	10.00	0.50	5.1	29.6	2.0	1.94
GT26	20.00	60.00	10.00	10.00	0.50	5.0	29.3	2.0	1.90
GT35	30.00	50.00	10.00	10.00	0.50	4.8	29.1	2.1	1.85
GT44	40.00	40.00	10.00	10.00	0.50	4.7	28.5	2.1	1.84
GT53	50.00	30.00	10.00	10.00	0.50	4.5	29.0	2.1	1.81
GT62	60.00	20.00	10.00	10.00	0.50	4.4	28.3	2.1	1.76
GT71	70.00	10.00	10.00	10.00	0.50	4.4	27.1	2.2	1.75
GT80	80.00	0	10.00	10.00	0.50	4.3	26.1	2.3	1.73

the glasses ΔT increases except for the sample with $x = 80$ (namely GT80). Thus, we can conclude that introducing appropriate amount of GeO_2 into this quaternary glass system can improve the glass thermal stability.

As well known, rare earth ions in solids do not necessarily emit photons since they can undergo a variety of non-radiative transitions. The most important one is multiphonon transitions from more than one bridged host phonon. Therefore, highest host phonon energy is a very influential factor for optical amplifiers to realize higher emission efficiency. Host phonon energy can be obtained by the phonon sideband (PSB) of Eu^{3+} ions and can be clearly observed on the high-energy side of $^7F_0 \rightarrow {}^5D_2$ transition [12]. Fig. 2 shows the compositional dependence of the phonon sideband of glass host $xGeO_2$–$(80-x)TeO_2$–10ZnO–10BaO. It can be seen that phonon energy of glass host increases with increasing GeO_2-content. The ternary glass system GT08 shows lowest phonon energy around 700 cm^{-1}. The low phonon energy is benefit to enhance the quantum efficiency of $^4I_{13/2} \rightarrow {}^4I_{15/2}$ transition, but it also causes an intense up-conversion emission due to the excited state absorption of $^4I_{11/2}$ state, which wastes the pumping energy. Thereby, properly adjusting phonon energy of the glass host can restrain the up-conversion emission and promote infrared emission originating from $^4I_{13/2} \rightarrow {}^4I_{15/2}$ transition. As seen in Fig. 2 the GeO_2 can be the candidate component for adjusting the phonon energy of the glass host. Choosing proper amount of GeO_2 can improve the emission efficiency (or external quantum efficiency) of $^4I_{13/2} \rightarrow {}^4I_{15/2}$ transition, though the quantum efficiency of $^4I_{13/2}$ probably decreases, nevertheless, higher emission efficiency is more important than the higher quantum efficiency.

The optical absorption edge is an important parameter for describing the solid state materials. It is necessary to realize the effect of the content of GeO_2 introduced into the tellurite glasses on optical absorption edge. The optical absorption edge for disordered materials is interpreted in terms of indirect transitions across an optical band gap. For the absorption by indirect transitions the absorption coefficient, $\alpha(\omega)$, is given by [13]

$$\alpha(\omega) = \frac{A(\hbar\omega - E_{OPT})^2}{\hbar\omega}, \quad (1)$$

where $\alpha(\omega)$ is the absorption coefficient, A is a constant, E_{OPT} is the optical band edge and $\hbar\omega$ is the photon energy of the incident radiation. The optical band edge is obtained by extrapolating from the linear region of the plots of $\hbar\omega$. Fig. 3 shows the compositional dependence of optical absorption band edge in GTEr glasses. The absorption edges of these glasses are in the region of 3.4–4.2eV.

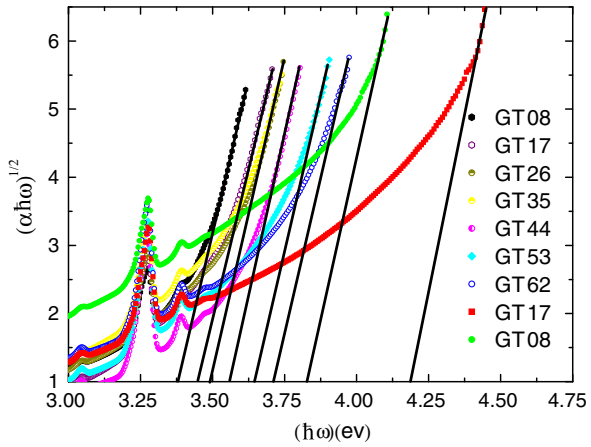

Fig. 3. The compositional dependence of optical energy gap in $xGeO_2$–$(80-x)$-TeO_2–10ZnO–10BaO glasses (x = 0–80 mol%).

Increasing the GeO_2-content will lead absorption edge to blue shift, contrarily, red shift will happen when the TeO_2-content increases.

In order to obtain the optical transition properties of Er^{3+} in these glasses with various compositions, Judd–Ofelt [14,15] analysis was performed. The Judd–Ofelt parameters for all the studied samples were calculated according to the standard computing procedure [16]. Fig. 4 shows the parameter dependence on the host composition. In this figure, the X-axis represents the content of GeO_2 and Y-axis displays the values of Ω_t (t = 2,4,6). It is found that with increasing GeO_2 content, Ω_4 hardly changes, Ω_6 decreases by a little, but Ω_2 increases first, and then decreases. The error in these calculations is less than 10. It is generally accepted that Ω_2 is related with the symmetry of the glass hosts and the covalency of the rare earth-ligand bond. Ω_6 is inversely proportional to the covalency of the rare earth-ligand bond [17,18]. According to the electronegativity theory [19], the smaller the difference of electronegativity between cation and anion ions, the stronger the covalency of the bond. The values of electronegativity, for Te, Ge and O elements, are 2.01, 2.02 and 3.5, respectively. As a result, the covalency of Ge–O bond is a little stronger than that of Te–O bond. With increasing GeO_2 content the influence of Ge–O bond on the local ligand environments around Er^{3+} ions increases, therefor Ω_6 value would decrease. Ω_2 is more sensitive to the evolution of the surroundings than Ω_6. With increasing GeO_2-content the influence of Ge–O bond on the local ligand environments around Er^{3+}

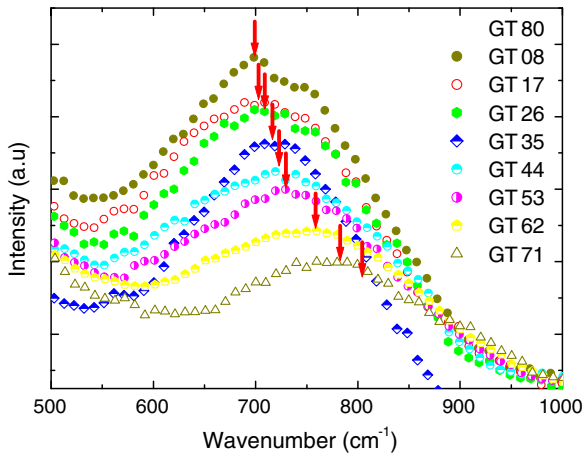

Fig. 2. The phonon sideband of glasses $xGeO_2$–$(80-x)TeO_2$–10ZnO–10BaO glasses (x = 0–80 mol%).

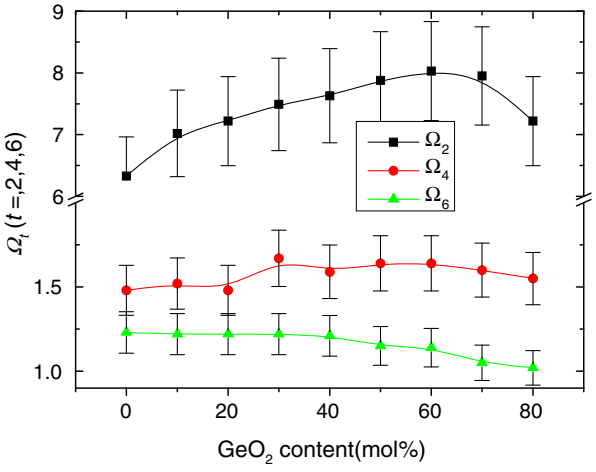

Fig. 4. The relationship between intensity parameters Ω_t (t = 2,4,6) and GeO_2 content in $xGeO_2$–$(80-x)TeO_2$–10ZnO–10BaO glasses (x = 0–80 mol%).

ions increases, the disordered degree of environment surrounding Er^{3+} become higher, thus, resulting the increase of Ω_2. When the content of GeO_2 increases up to 60% the glass shows the property of germanate glass and the disordered degree of environment surrounding Er^{3+} decreases and hence Ω_2 would decrease as seen in Fig. 4.

4. Discussion

As mentioned above the tellurite glass having lower phonon energy than that of germanate usually exhibit intense up-conversion emission consuming the pumping energy, so effective elimination of up-conversion emission is beneficial to the infrared emission.

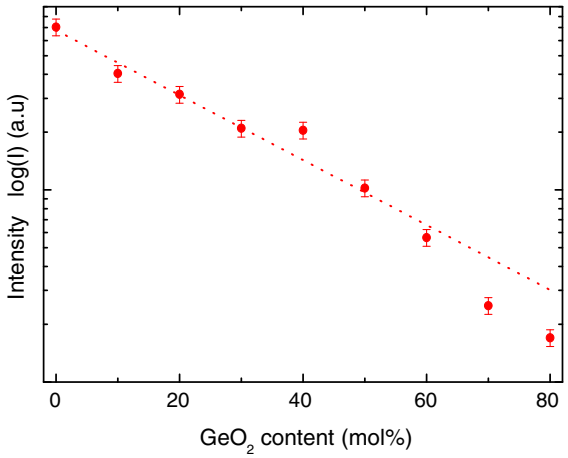

Fig. 5. The relationship between green up-conversion emission intensity of Er^{3+} ions under 980 nm excitation and GeO_2 content in $xGeO_2$–$(80-x)TeO_2$–10ZnO–10BaO glasses (x = 0–80 mol%).

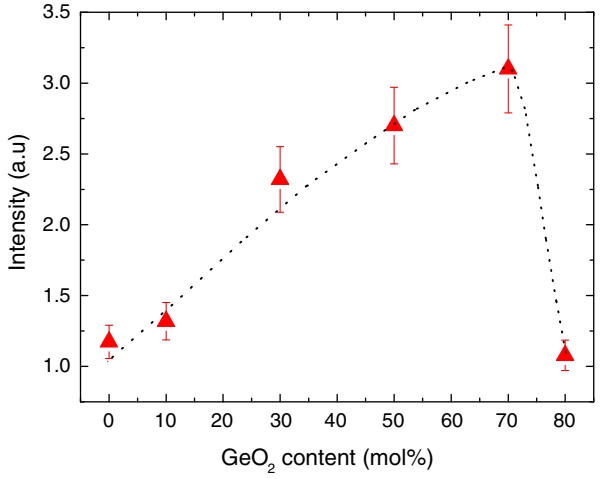

Fig. 6. The relationship between the intensity of $^4I_{13/2}$–$^4I_{15/2}$ emission of Er^{3+} ions under 980 nm excitation and GeO_2 content in $xGeO_2$–$(80-x)TeO_2$–10ZnO–10BaO glasses (x = 0–80 mol%).

Fig. 5 shows the relationship between green up-conversion emission intensity of Er^{3+} ions and GeO_2 content under 980 nm excitation. It can be seen that with increasing GeO_2-content the green up-conversion emission intensity of Er^{3+} ions decreases quasi-exponentially. Fig. 6 shows the relationship between the emission intensity of $^4I_{13/2} \rightarrow {}^4I_{15/2}$ transition and GeO_2-content under 980 nm excitation. It can be seen that with increasing GeO_2 content the emission intensity of $^4I_{13/2} \rightarrow {}^4I_{15/2}$ of Er^{3+} ions first increases and reach its maximum at 70% of GeO_2-content, and then goes down. From Figs. 5 and 6, it can be deduced that introducing GeO_2 into tellurite glasses leads to increasing the non-radiative relaxation rate from $^4I_{11/2}$ level to $^4I_{13/2}$ level, decreasing excited state absorption of $^4I_{11/2}$ level and improving emission intensity of $^4I_{13/2}$ level of Er^{3+} ions. In the glass with 80% GeO_2 (a pure germinate glass), the intensity of $^4I_{13/2} \rightarrow {}^4I_{15/2}$ transition decreases, this is probably due to its high phonon energy (see Fig. 2) which would cause an intensified non-radiative relaxation from $^4I_{13/2}$ level to $^4I_{15/2}$ level; meanwhile, compared with the Er^{3+}-doped telurite glass, Er^{3+}-doped germinate glass usually displays intense red up-conversion emission [20,21] originating from the excited state absorption from $^4I_{13/2}$ level to $^4F_{9/2}$ level, thus resulting in a decrease of the 1.5 μm emission. In order to clarify this fact, further experimental study would be needed.

According to Judd–Ofelt expression the radiative relaxation rate A_{rad} for the Er^{3+}:$^4I_{13/2} \rightarrow {}^4I_{15/2}$ can be deduced as following form [21]

$$A_{rad} = \frac{16\pi^3 v^3 e^2}{3hc^3\varepsilon_0(2J+1)}\left[\frac{n(n^2+2)^2}{9}(0.019\Omega_2 + 0.118\Omega_4 + 1.462\Omega_6) + \frac{n^3}{4m^2c^2}|\langle f^N\psi J|L+2S|f^N\psi' J'\rangle|^2\right]. \quad (2)$$

Because of the little contribution of Ω_2 and Ω_4 to the value of A_{rad}. Eq. (2) can be simplified as

$$A_{rad} = \frac{16\pi^3 v^3 e^2}{3hc^3\varepsilon_0(2J+1)}\left[\frac{1.462n(n^2+2)^2}{9}\Omega_6 + \frac{n^3}{4m^2c^2}|\langle f^N\psi J|L+2S|f^N\psi' J'\rangle|^2\right], \quad (3)$$

where $\langle f^N\psi J|L+2S|f^N\psi' J'\rangle$ are the reduced matrix elements of the operator $L+2S$, which are host independent parameters. Because Ω_6 has a little change (shown in Fig. 4) the radiative relaxation rate A_{rad} is mainly decided by the refractive indexes n. In Table 1 it shows that with increasing GeO_2-content the refractive indexes, n, decreases. Consequently, the radiative transition rate A_{rad} decreases with increasing GeO_2 content (see Table 2).

As well known the quantum efficiency η for a certain level of rare earth ions can be depicted as [22]

$$\eta = \tau_f A_{rad}, \quad (4)$$

where τ_f denotes the fluorescent lifetime of $^4I_{13/2}$ level. Table 2 shows the radiative transition rate A_{rad}, lifetime τ_f and quantum efficiency η of $^4I_{13/2}$ level in $xGeO_2$–$(80-x)TeO_2$–10ZnO–10BaO glasses. It is seen that with increasing GeO_2 content quantum efficiency η of $^4I_{13/2}$ level decreases. However, the intensified emission for $^4I_{13/2} \rightarrow {}^4I_{15/2}$ transition has been observed with the increase of the GeO_2-content. The intensified emission owes to the partial

Table 2
Radiative relaxation rate A_{rad}, fluorescent lifetime τ_f and quantum efficiency η of $^4I_{13/2}$ level in $xGeO_2$–$(80-x)TeO_2$–10ZnO–10BaO glasses (x = 0–80)

Sample	Error (%)	GT08	GT17	GT26	GT35	GT44	GT53	GT62	GT71	GT80
τ_f (ms)	1	2.94	3.08	3.17	3.19	3.26	3.53	3.83	4.04	4.19
A_{rad} (1/s)	10	340	324	307	278	270	249	226	210	193
η (%)	10	100	99.7	97.2	88.6	88.1	87.8	86.4	84.9	81.0

elimination of up-conversion emission, and the increase of pumping efficiency because the increase of the GeO_2-content can effectively decrease the population of the $^4I_{11/2}$ level and effectively populate $^4I_{13/2}$ level at the same time.

5. Conclusions

A series of new glasses with composition xGeO$_2$–(80 − x)TeO$_2$–10ZnO–10BaO (x = 0–80, with an increment of 10) were prepared by using the melt-quenching technique. On the basis of DTA and optical absorption band edge data, it was suggested that introducing GeO_2 into tellurite glass improved the thermal stability and made a blue shift of the optical absorption edge of host matrix. The increased emission intensity of $^4I_{13/2}$ level and decreased up-conversion emission indicated that introducing proper GeO_2-content into tellurite glasses improved 1.5 μm emission efficiency, though introducing GeO_2 led to a decrease of radiative relaxation rate A_{rad} and quantum efficiency of $^4I_{13/2}$ level. It is expected that Er^{3+}-doped GeO_2–TeO_2–ZnO–BaO glass would be a good candidate for optical amplifier.

Acknowledgments

This work was partially supported by the National Natural Science Foundation of China (50572102, 50502131), and Natural Science Foundation of Jilin Province (1999514, 20030514-2) and Outstanding Young People Foundation of Jilin Province (20040113), The Joint Program of NSFC (National Natural Science Foundation of China)-GACAC (General Administration of Civil Aviation of China) (Grant No. 60776814).

References

[1] V.K. Tihomirov, D. Furniss, A.B. Seddon, Appl. Phys. Lett. 81 (11) (2002) 1937.
[2] J.S. Wang, E.M. Vogel, E. Snitzer, Opt. Mater. 3 (1994) 863.
[3] S. Tanabe, N. Sugimoto, S. Ito, T. Hanada, J. Lumin. 87 (2000) 670.
[4] Q.P. Chen, M. Ferraris, D. Milanese, Y. Menke, E. Monchiero, G. Perrone, J. Non-Cryst. Solids 324 (2003) 12.
[5] M. Benatsou, M. Bouazaoui, Opt. Mater. 137 (1997) 143.
[6] C. Jiang, P.Z. Deng, J.Z. Zhang, F.X. Gan, Phys. Lett. A 324 (2004) 91.
[7] X. Feng, S. Tanabe, T. Hanada, J. Non-Cryst. Solids 48 (2001) 281.
[8] Z. Pan, S.H. Morgan, J. Lumin. 75 (1997) 301.
[9] G. Nunzi Conti, V.K. Tikhomirov, B. Chen, S. Berneschi, M. Brenci, S. Pelli, A.B. Seddon, M. Bettinelli, A. Speghini, G.C. Righini, Proc. SPIE 4990 (2003) 97.
[10] L.L. Neindre, S.B. Jiang, B.C. Hwang, T. Luo, J. Watson, J. Non-Cryst. Solids 255 (1999) 97.
[11] M.G. Drexhage, O.H. Ei Bayoumi, C.T. Moyniyan, J. Am. Ceram. Soc. C 65 (1982) 168.
[12] S. Tanabe, S.T. Hirao, N. Soga, J. Non-Cryst. Solids 122 (1990) 59.
[13] C. Ance, F. De Chelle, J.P. Ferraton, J. Non-Cryst. Solids 91 (1987) 243.
[14] B.R. Judd, Phys. Rev. 127 (1962) 750.
[15] G.S. Ofelt, J. Chem. Phys. 37 (1962) 511.
[16] A.S.S. Camargo, L.A.O. Nunes, I.A. Santos, D. Garcia, J.A. Eiras, J. Appl. Phys. 95 (2004).
[17] S. Tanabe, J. Non-Cryst. Solids 1 (1999) 259.
[18] S. Tanabe, J. Appl. Phys. 73 (1993) 8451.
[19] L. Pauling, J. Am. Chem. Soc. 51 (1929) 1010.
[20] Z. Jin, Q. Nie, T. Xu, S. Dai, X. Shen, X. Zhang, Mater. Phys. Chem. 104 (2007) 62.
[21] L. Lu, Q. Nie, X. Shen, S. Dai, T. Xu, Spectrochim. Acta Part A 67 (2007) 1228.
[22] D.K. Sardar, W.M. Bradley, J.J. Perez, J.B. Gruber, J. Appl. Phys. 93 (2003) 2602.